Spectrochimica Acta Part A: Molecular and Biomolecular Spectroscopy 226 (2020) 117645

Contents lists available at ScienceDirect

Spectrochimica Acta Part A: Molecular and Biomolecular Spectroscopy

journal homepage: www.elsevier.com/locate/saa

A dual–function fluorescent probe for Hg (II) and Cu (II) ions with two mutually independent sensing pathways and its logic gate behavior

Ming Dong*, Jinyu Tang, Yanfei Lv, Yating Liu, Jinfeng Wang, Tiantian Wang, Jingyi Bian, Chunju Li**

Tianjin Key Laboratory of Structure and Performance for Functional Molecules, MOE Key Laboratory of Inorganic–Organic Hybrid Functional Material Chemistry, College of Chemistry, Tianjin Normal University, Tianjin, 300387, PR China

ARTICLE INFO

Article history:
Received 12 June 2019
Received in revised form
10 September 2019
Accepted 8 October 2019
Available online 9 October 2019

Keywords:
Dual–function
Ratiometric
Chemodosimeter
Combinatorial logic circuit

ABSTRACT

A dual–function fluorescent **Probe 1** has been synthesized conveniently by coupling rhodamine hydrazone with *O*–vinyl protected hydroxyl benzaldehyde. **Probe 1** was a highly selective and sensitive chemodosimeter for Hg^{2+} through specific hydrolysis reaction of vinyl ethers with significant fluorescence quenching in CH_3CN–PBS buffer (3:7, v/v) solution. Meanwhile, **Probe 1** showed a ratiometric fluorescent detection of Cu^{2+} with a remarkable large Stokes shift (150 nm) by the opening of the spirolactam ring in CH_3CN–PBS buffer (3:7, v/v) solution. Hence, the two recognition mechanisms realized well by using a single fluorescent probe. Moreover, **Probe 1** could be efficiently applied to the combinatorial logic circuit of NOR and INHIBIT gates through the procured spectral results, respectively.

1. Introduction

Many metal ion analytes play a vital role in various biological processes, beyond an optimum limit each of them could potentially become dangerous to human beings. This makes the sensing and analysis of such analytes very important. Even at low concentrations, Hg^{2+} can lead to the dysfunction of the brain, kidney, and central nervous system because biological ligands, especially for sulfur-containing proteins, DNA, and enzymes, can coordinate with mercury cations [1–3]. The permitted limit of Hg^{2+} ion in water is only 2 ppb as per the U.S. EPA [4]. Thus, mercury pollution has sparked interest in the design of new strategies to monitor Hg^{2+} in biological and environmental samples. Since Czarnik demonstrated the first synthetic chemodosimeter for the selective determination of Hg^{2+} [5], many new approaches based on the irreversible chemical reaction have emerged [6,7].

Copper, one of the essential elements for life, is a cofactor of numerous enzymes and plays a crucial role in many biological processes [8]. This redox reactivity is potentially harmful to live organisms, since compromises in homeostatic control of copper pools may result in oxidative damage to tissue and organ systems [9]. The permitted limit of Cu^{2+} ion in water is only 1.3 ppm as per the U.S. EPA [10]. Thus, developing a highly selective method to detect Cu^{2+} is imminently required, and a great number of fluorescent probes for selective detection of Cu^{2+} ions [11–19] have been prepared.

Compared to single–analyte responsive probes, multifunctional probes [20–33] that can simultaneously detect multiple analytes exhibit advantages such as analytical time reduction, convenience, and cost–effectiveness. Though there are several reports based on rhodamine systems for the detection of Hg^{2+} or Cu^{2+}, no effort has been made to detect both Hg^{2+} and Cu^{2+} ion simultaneously. Herein we report a new dual–function fluorescent **Probe 1** (Scheme 1) for the detection of Hg^{2+} and Cu^{2+} using two different mutually independent sensing pathways. **Probe 1** was a highly selective and sensitive chemodosimeter for Hg^{2+} through specific hydrolysis reaction of vinyl ethers with significant fluorescence quenching in CH_3CN–PBS buffer (3:7, v/v) solution. Meanwhile, **Probe 1** showed a ratiometric fluorescent detection of Cu^{2+} with a remarkable large Stokes shift (160 nm) by the fluorescence resonance energy transfer (FRET) from vinyl protected 4-diethylamino aryl to rhodamine fluorophore in CH_3CN–PBS buffer (3:7, v/v) solution. The single fluorescent molecule **Probe 1**, can respond to Hg^{2+}, Cu^{2+}, and Hg^{2+}/Cu^{2+} with three different sets of fluorescence signals (Table 1). Correspondingly, **Probe 1** exhibited NOR and INHIBIT logic gates with Hg^{2+} and Cu^{2+} as chemical inputs by monitoring the emission mode at 515 and 580 nm, respectively, due to the two different mutually independent sensing pathways.

* Corresponding author.
** Corresponding author.
E-mail addresses: hxxydongm@tjnu.edu.cn (M. Dong), cjli@shu.edu.cn (C. Li).

https://doi.org/10.1016/j.saa.2019.117645
1386-1425/

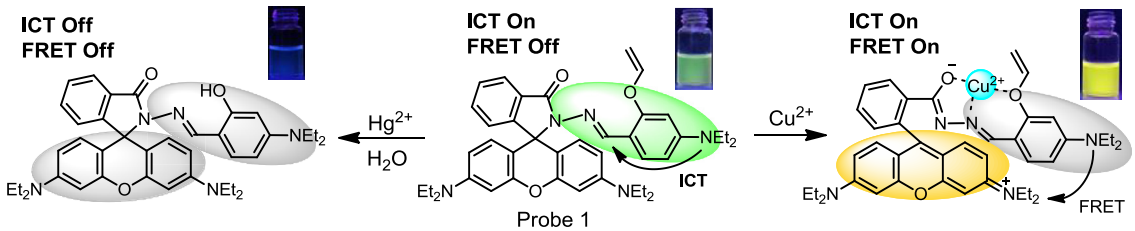

Scheme 1. Dual–function fluorescent **Probe 1** for the detection of Hg^{2+} and Cu^{2+} using two different mutually independent sensing pathways.

Table 1
A unique type of a single fluorescent probe that can report Cu^{2+}, Hg^{2+}, and Cu^{2+}/Hg^{2+} with three different sets of fluorescence signals: black-yellow-yellow; black–black–black; and black–black–yellow.

Input	Ex. 420 nm		Ex. 530 nm	Fluorescence singal patterns
	Em. 515 nm	Em. 580 nm	Em. 580 nm	
Free				Cyan-black-black
Cu^{2+}				Black-yellow-yellow
Hg^{2+}				Black- black - black
$Cu^{2+} + Hg^{2+}$				Black- black -yellow

2. Experiment

2.1. Materials and instruments

Unless otherwise noted, all chemicals and solvents were obtained as the analytical grade by commerce and used without further purification. Flash chromatography was carried out using 200–300 mesh silica gel. ^{1}H and ^{13}C NMR spectra were recorded in $CDCl_3$ or DMSO-d_6 using a Bruker 400 MHz instrument and spectral data are reported in ppm relative to tetramethylsilane (TMS) as an internal standard. Fluorescence emission spectra were recorded on a Hitachi F4500 fluorescence spectrofluorometer. The pH value was measured using a Sartorius PB–10 pH meter equipped with a PY–ASI combination glass pH electrode.

Stock solutions (10.0 mM) of the perchlorate salts of Mg^{2+}, Ca^{2+}, Ba^{2+}, Sr^{2+}, Ni^{2+}, Cr^{3+}, Mn^{2+}, Co^{2+}, Zn^{2+}, Cd^{2+}, Pb^{2+}, Fe^{2+}, Fe^{3+}, Cu^{2+} and Hg^{2+} were prepared in deionised water. Stock solution (10.0 mM) of Cu^{+} ions was generated from $CuSO_4$ (10.0 mM) and NaAsc (Sodium ascorbate, 100 mM) in situ [34].

Stock solutions of the host compounds (10.0 mM) were prepared in CH_3CN. Test solutions were prepared by diluting 2.0 μL of **probe 1** stock solution to 2.0 mL with CH_3CN–PBS buffer (10.0 mM, pH = 7.40, 3/7, v/v) solution, followed by the addition of an appropriate aliquot of each ion stock solution. For all measurements, fluorescence spectra were obtained by excitation at 420 or 530 nm; both the excitation and emission slit widths were 5 nm. Fluorescence quantum yields were determined by standard methods, using quinine sulfate ($\Phi = 0.54$ in 1 N H_2SO_4) as a standard.

2.2. Preparation of probe 1

Compound **1**–**3** were synthesized according to literature [35,36], as shown in Scheme 2. A stirred solution of **2** (0.219 g, 1 mmol), **3** (0.456 g, 1 mmol), and 50 mL ethanol was heated to reflux for 6 h. After the ethanol was evaporated under reduced pressure, the residue was purified by silica gel column chromatography (CH_2Cl_2/MeOH = 100:1, v/v) to give 0.52 g of **Probe 1** (79%) as a yellow solid (Figs. S1 and S2). ^{1}H NMR ($CDCl_3$, 400 MHz): δ 8.49 (s, 1H), 7.98 (m, 2H), 7.84 (d, J = 8.8 Hz, 1H), 7.42 (m, 2H), 7.06 (m, 1H), 6.54 (d, J = 8.8 Hz, 2H), 6.41 (dd, J = 13.6, 6.0 Hz, 1H), 6.40 (d, J = 2.4 Hz, 2H), 6.34 (dd, J = 8.8, 2.4 Hz, 1H), 6.21 (dd, J = 8.8, 2.4 Hz, 1H), 6.02 (d, J = 2.4 Hz, 1H), 4.51 (dd, J = 13.6, 1.6 Hz, 1H), 4.20 (dd, J = 6.0, 1.6 Hz, 1H), 3.30 (m, 12H), 1.14 (t, J = 7.2 Hz, 12H), 1.11 (t, J = 7.2 Hz, 6H); ^{13}C NMR ($CDCl_3$, 100 MHz): δ 164.8, 163.9, 152.7 (2C), 152.2, 150.9, 149.5, 148.8 (2C), 142.0, 132.8, 132.1, 129.1, 128.0, 127.9 (2C), 127.8 (2C), 123.4, 123.1, 114.1, 109.5, 108.1 (2C), 106.2, 103.8, 98.0 (2C), 65.6, 44.5 (2C), 44.3 (4C), 12.6 (4C), 12.5 (2C). ESI–MS: m/z = 658.35 $[M + H]^{+}$.

3. Results and discussion

3.1. Fluorescent response to Cu^{2+} and Hg^{2+}

Probe 1 showed good stability in pH ranging from 7.0 to 10.0 (Fig. S3). Upon the addition of Cu^{2+}, **probe 2** exhibited good fluorescence response for Cu^{2+} in the pH range of 5.0–10.0. Considering the applications in biological systems, pH 7.40 was selected for the following experiments.

As shown in Fig. 1a, **Probe 1** exhibited a weak emission band at 580 nm by excitation of the rhodamine fluorophore at 530 nm. Then Mg^{2+}, Ca^{2+}, Ba^{2+}, Sr^{2+}, Ni^{2+}, Cr^{3+}, Mn^{2+}, Co^{2+}, Zn^{2+}, Cd^{2+}, Pb^{2+}, Fe^{2+}, Fe^{3+}, Cu^{+}, Cu^{2+} and Hg^{2+} ions were used to examine the selectivity of **Probe 1** (10 μM) in CH_3CN–PBS buffer (10.0 mM, pH = 7.40, 3/7, v/v) solution, and F^{-}, Cl^{-}, Br^{-}, I^{-}, CN^{-}, AcO^{-}, ClO_4^{-}, $CF_3SO_3^{-}$, NO_3^{-}, HSO_4^{-}, $H_2PO_4^{-}$, BF_4^{-}, N_3^{-}, and SCN^{-} (as corresponding tetrabutylammonium salt, respectively) were used to study the effect of counter anion in the sensing. Fluorescence spectra were recorded after 5 min upon the addition of 5.0 equiv of each of the respective ions. Compared to other ions measured, only Cu^{2+}

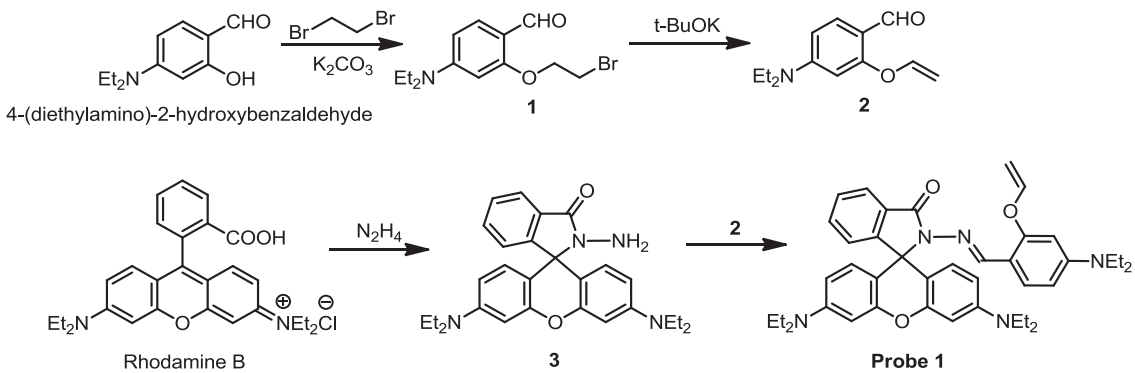

Scheme 2. The synthesis of **Probe 1**.

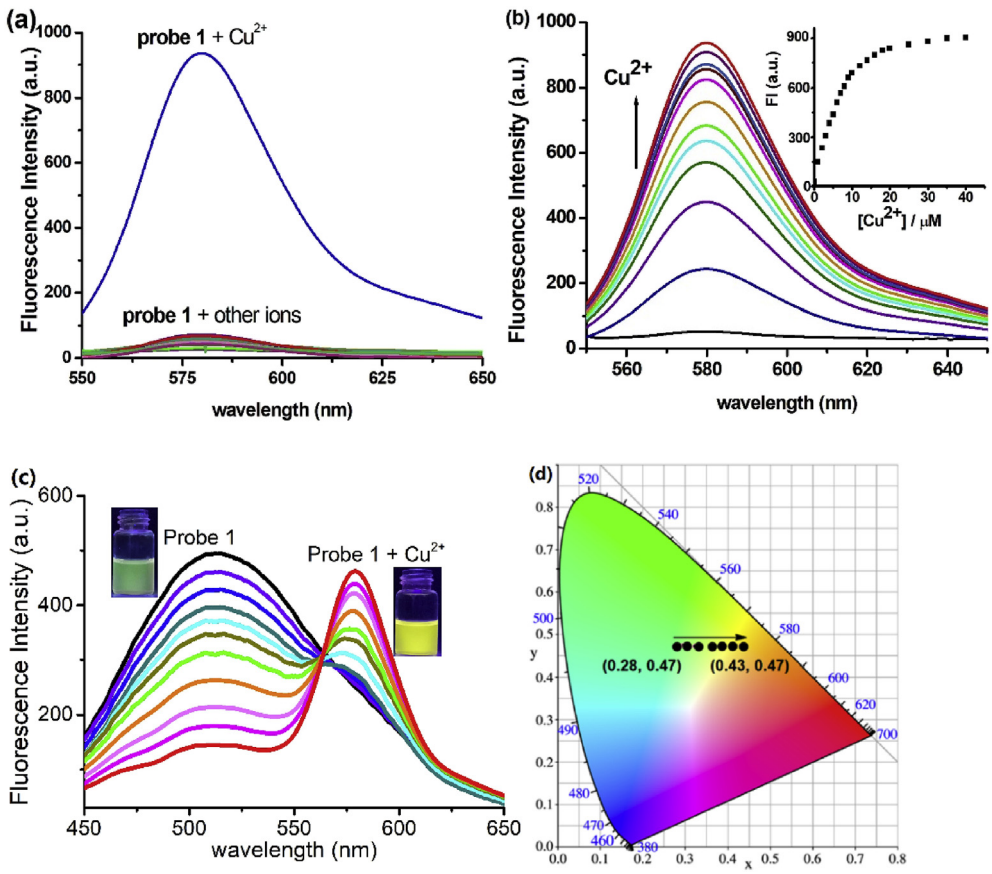

Fig. 1. (a) Fluorescence responses of **Probe 1** (10 μM) in CH_3CN–PBS buffer (10.0 mM, pH = 7.40, 3/7, v/v) solution (λ_{ex} = 530 nm). (b) Fluorescent spectra of **Probe 1** (10 μM) upon addition of Cu^{2+} (from 0 to 4.0 equiv) in CH_3CN–PBS buffer (10.0 mM, pH = 7.40, 3/7, v/v) solution (λ_{ex} = 530 nm). Inset: Plot of the fluorescent intensity of **Probe 1** as a function of Cu^{2+} concentration at 580 nm. (c) Fluorescent spectra of **Probe 1** (10 μM) upon addition of Cu^{2+} in CH_3CN–PBS buffer (10.0 mM, pH = 7.40, 3/7, v/v) solution (λ_{ex} = 420 nm). (d) Fluorescence changes in the CIE diagram of **Probe 1** (10 μM) with the increase of Cu^{2+} in the CH_3CN–PBS buffer solution. λ_{ex} = 420 nm.

brought about a prominent fluorescence emission band centered at 580 nm assigned as a characteristic peak of ring–opened rhodamine moiety, which indicated that **Probe 1** displayed selective fluorescence response to Cu^{2+}. To validate the selectivity of **Probe 1** in practice, the competition experiments were also conducted by addition of 5.0 equiv of Cu^{2+} to their aqueous solutions in the presence of 10.0 equiv of other metal ions (Fig. S4). There is no obvious interference for each of the competitive metal ions, which indicated that the system of **Probe 1**–Cu^{2+} was hardly affected by these coexistent ions. These results suggested that **Probe 1** revealed an excellent selectivity toward Cu^{2+} in CH_3CN–PBS buffer at neutral pH.

The fluorescence titrations of Cu^{2+} were also studied using a 10.0 μM solution of **Probe 1** in CH_3CN–PBS buffer (10.0 mM, pH = 7.40, 3/7, v/v) solution when excited at 420 and 530 nm, respectively (Fig. 1b and c). Upon the addition of Cu^{2+} to the solution of **Probe 1** (Φ = 0.08), a remarkable increase of the fluorescence intensity (Φ = 0.21) at 580 nm with 21–fold was observed by excitation at 530 nm. Further increase in the concentration of Cu^{2+} (>30 μM) led to no further fluorescence increase (Fig. 1b, inset).

Furthermore, by excitation at 420 nm, Cu^{2+} caused the change of the maximum fluorescence emission of **Probe 1** from 515 to 580 nm, upon the addition of Cu^{2+} to the solution, which indicated a clear ratiometric fluorescence change (Fig. 1c). The ratio of fluorescence intensity at 580 and 515 nm increased linearly with the concentration of Cu^{2+} (2.0–25.0 μM, Fig. S5).

The corresponding detection limit for Cu^{2+} was calculated to be 0.67 μM (42.6 ppb), as shown in Fig. S6. Meanwhile, the solution containing Cu^{2+} exhibited a change of fluorescence color from cyan to yellow under irradiation by a 365 nm UV lamp (as shown in Fig. 1c), which were also marked in the CIE diagram. It is worth mentioning that the CIE color coordinates of Probe 1 were located at the boundary between the green light and yellow light. The Job's plots and nonlinear fitting of the titration curve (Figs. S7 and S8) confirmed a 1:1 stoichiometry between **Probe 1** and Cu^{2+} with the association constants of $1.4 \times 10^6\ M^{-1}$. Reversible titration using EDTA/Cu^{2+} (Fig. S9) demonstrated that the above fluorescent responses were also reversible. These results indicated that Probe1 could be a fluorescent ratiometric probe for the Cu^{2+} ion in the CH_3CN–PBS buffer solution.

We surmised that the response of **Probe 1** to Hg^{2+} is feasible owing to specific hydrolysis reaction of vinyl ethers. Upon the addition of various metal ions to the CH_3CN–PBS buffer (10.0 mM, pH = 7.40, 3/7, v/v) solution of **Probe 1**, a significant decrease of the fluorescence intensity ($\Phi = 0.005$) at 515 nm was observed (Fig. 2a). The fluorescence intensity of **Probe 1** at 515 nm decreased to 24% when 10.0 equiv of Hg^{2+} was present. The fluorescence quench could be due to the hydrolysis reaction of aryl vinyl ethers promoted by Hg^{2+}, which may result in the inhibition of intramolecular charge transfer (ICT). The competition experiments were also conducted by addition of 4.0 equiv of Hg^{2+} to the aqueous solutions in the presence of 10.0 equiv of other metal ions (Fig. S10). There is no obvious interference for each of the competitive metal ion. When the fluorescence spectra were recorded after 60 min (Fig. S11), upon the addition of Hg^{2+} to the solution of **Probe 1**, the titration of **Probe 1** with Hg^{2+} (from 0 to 2.5 equiv.) showed saturation behavior at 0.5 equiv. of Hg^{2+}, and suggested that **Probe 1** could be a chemodosimeter for Hg^{2+} with the 1:1 stoichiometry between **Probe 1** and Hg^{2+}.

The fluorescence titrations of Hg^{2+} were also studied using a 10.0 μM solution of **Probe 1** in CH_3CN–PBS buffer (10.0 mM, pH = 7.40, 3/7, v/v) solution when excited at 420 nm (Fig. 2b). Upon the addition of Hg^{2+} to the solution for 5 min, a remarkable decrease of the fluorescence intensity at 515 nm was observed. Further increase in the concentration of Hg^{2+} (>40 μM) led to no further fluorescence increase (Fig. 2b, inset). The corresponding detection limit for Hg^{2+} was calculated to be 1.22 μM (244 ppb), as shown in Fig. S12.

3.2. Proposed mechanism

The photophysical properties revealed that **Probe 1** was a highly selective and sensitive chemodosimeter for Hg^{2+} and a ratiometric fluorescent probe for Cu^{2+} simultaneously. More direct evidence was obtained by the ^1H NMR titrations (Fig. 3) and the ESI mass spectrum (Fig. S13) of the system of **Probe 1**–Hg^{2+}. As shown in Fig. 3, H_a, H_b, and H_c belong to the proton signals of vinyl ether moiety in **Probe 1** (Fig. 3c). Remarkably, these signals disappeared after the addition of Hg^{2+} (Fig. 3b), and instead, the imine moiety and phenolic hydroxyl group proton signals of the compound 4 were observed. In mass spectrum, a peak at *m/z* 934.99 was assigned to oxymercuration intermediate **Probe 1**–$\mathbf{Hg^{2+}}$ (Fig. S13). Accordingly, upon the addition of Hg^{2+} to the solution of **Probe 1**, the Hg^{2+}–promoted hydrolysis reaction of aryl vinyl ether occurred, followed by the generation of phenol hydroxyl, which is a weaker electron-donating group than vinyl ether group [37]. Then the decrease of the fluorescence intensity at 515 nm may be due to breaking the ICT process (Intramolecular Charge Transfer) from 4-diethylamino group to imine moiety.

A plausible mechanism of **Probe 1** for detecting Cu^{2+} is proposed in Fig. 4, in which Cu^{2+} is coordinated cooperatively with carbonyl O, imino N, and the ortho-phenol O, and induced ring–opening of the spirolactam moiety.

This mechanism has been researched in detail by Tong's work [38]. That suggests **Probe 1** could be served as a ratiometric fluorescent chemosensor with the FRET from the 4-diethylamino aryl (donor) to the ring–opened form of rhodamine (acceptor), which is consistent with the photophysical properties (Fig. S14).

3.3. Logic behavior of probe 1 with Cu^{2+} and Hg^{2+} as inputs

Due to the distinguishing fluorescence responses of **Probe 1** (10.0 μM) in the presence of Cu^{2+} (20.0 μM) and Hg^{2+} (20.0 μM), it would be able to act as a two output combinatorial logic circuit. The combination of Cu^{2+} and Hg^{2+} as input signals on **Probe 1** led to a logic operation characteristic for a two–input INHIBIT gate on the emission at 580 nm and NOR gate on emission at 515 nm. As shown in Fig. 5, the fluorescence of **Probe 1** at 515 nm (output 1) is the strongest in the absence of any input, while the remaining combinations lead to a much weaker signal. Defining positive logic for the output 1 channel (binary encoding: high signal = 1, low signal = 0), the truth table of a NOR gate was gained. On the other

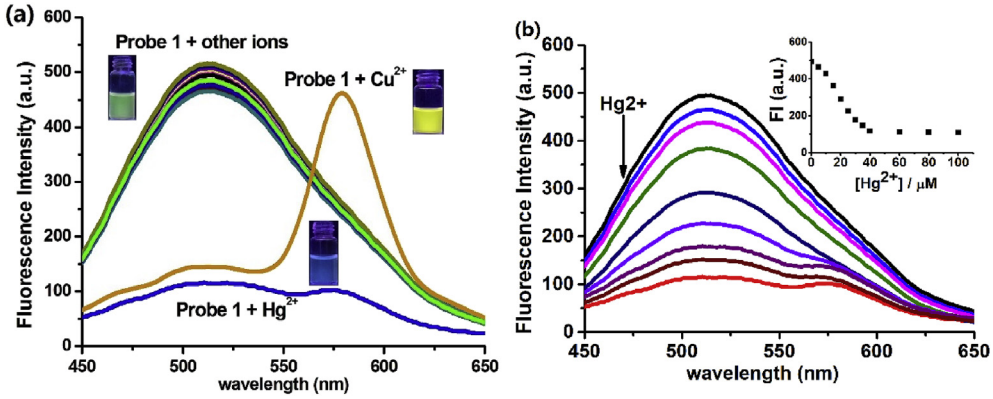

Fig. 2. (a) Fluorescence responses of **Probe 1** (10 μM) in CH_3CN–PBS buffer (10.0 mM, pH = 7.40, 3/7, v/v) solution (λ_{ex} = 420 nm). (b) Fluorescent spectra of **Probe 1** (10 μM) upon addition of Hg^{2+} (from 0 to 10.0 equiv) in CH_3CN–PBS buffer (10.0 mM, pH = 7.40, 3/7, v/v) solution (λ_{ex} = 420 nm). Inset: Plot of the fluorescent intensity of **Probe 1** as a function of Hg^{2+} concentration at 515 nm.

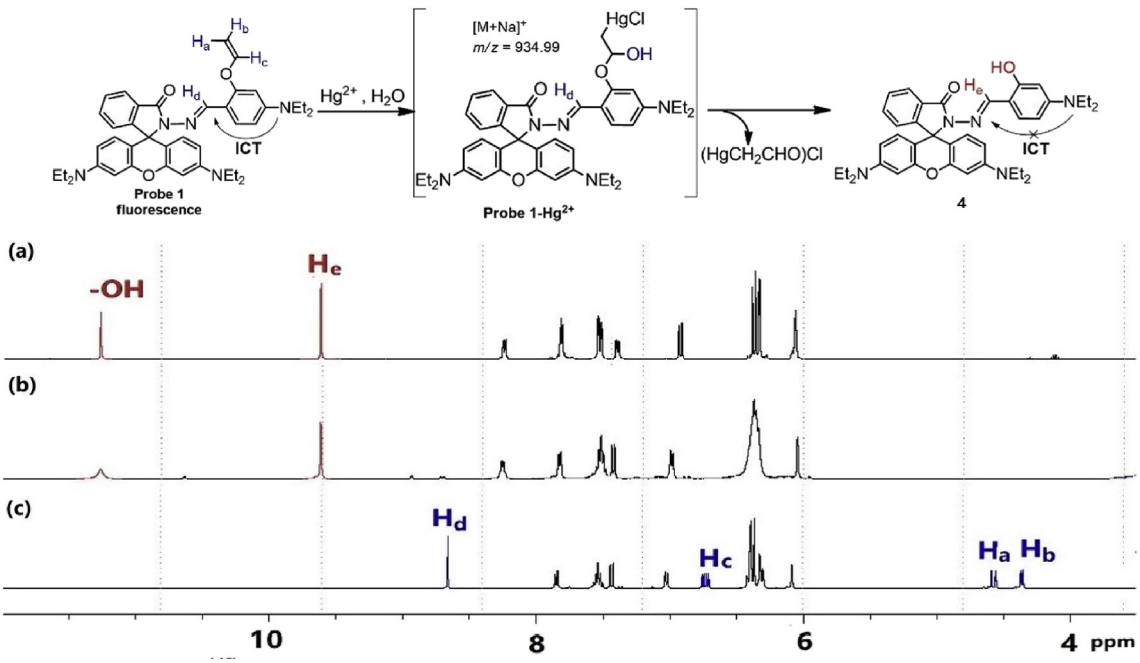

Fig. 3. Proposed mechanism of **Probe 1** with Hg^{2+} and Partial 1H NMR spectra in DMSO-d_6/D2O (10:1, v/v): (a) compound **4**, (b) **Probe 1** + Hg^{2+}, (c) probe 2 only.

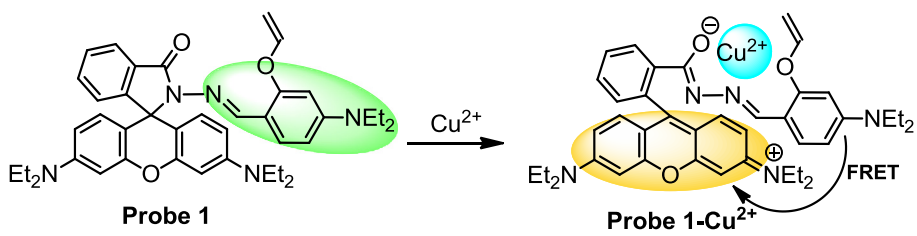

Fig. 4. Proposed binding mode between **Probe 1** and Cu^{2+}.

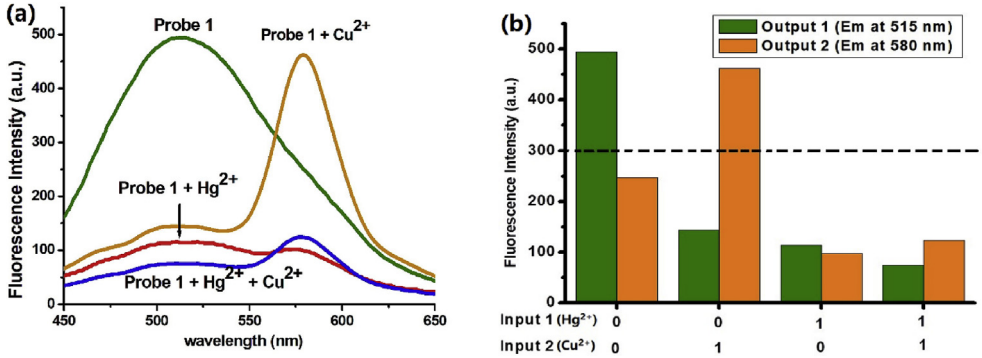

(c)

Input 1	Input 2	Output 1	Output 2
Hg^{2+}	Cu^{2+}	Emission at λ_{em}=515 nm	Emission at λ_{em}=580nm
0	0	1	0
0	1	0	1
1	0	0	0
1	1	0	0

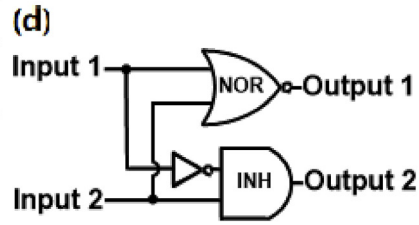

Fig. 5. (a) Input−dependent changes of fluorescence spectra of **Probe 1** with excitation at 420 nm. (b) The changes in fluorescence intensity of **Probe 1** (20.0 μM) at 515 and 580 nm with Cu^{2+} (20.0 μM) and Hg^{2+} (20.0 μM) as chemical inputs. (c) Truth table of **Probe 1**. Input 1 and Input 2 represent Hg^{2+} ions and Cu^{2+} ions (20.0 μM), respectively; Output 1 and Output 2 are the fluorescence intensity at 515 and 580 nm, respectively. (d) Scheme of the logic gate for **Probe 1**.

hand, the output 2 channel (emission at 580 nm) realizes an INHIBIT gate (binary encoding: high signal = 1, low signal = 0) with input 1 holding a veto. The strongest signal for the output 2 channel is observed in the presence of Cu^{2+}, and it is due to the FRET occurring within **Probe 1**–Cu^{2+} complex.

4. Conclusion

In summary, dual–function fluorescent **Probe 1** for the detection of Hg^{2+} and Cu^{2+} using two different mutually independent sensing pathways with excellent high selectivity has been successfully designed and synthesized. It exhibited a typical FRET process induced by Cu^{2+} and exhibited a significant change in the intensity ratio of the two emission bands of 4-diethylamino aryl and rhodamine, which is due to Cu–chelating spirolactam ring–open and efficiently transfer the energy from 4-diethylamino aryl to rhodamine. However, **Probe 1** employed Hg^{2+}–promoted hydrolysis reaction of aryl vinyl ethers and ICT strategies to realize a chemodosimeter for Hg^{2+}. Moreover, the combination of Cu^{2+}/Hg^{2+} as chemical inputs led to the realization of the combinatorial logic circuit of NOR and INHIBIT gates through the procured spectral results.

Declaration of competing interest

There are no conflicts of interest to declare.

Acknowledgment

This work was financially supported by the Doctoral Fund Project of Tianjin Normal University (52XB1407), and the Foundation of Development Program of Future Expert in Tianjin Normal University (WLQR201710).

Appendix A. Supplementary data

Supplementary data to this article can be found online at https://doi.org/10.1016/j.saa.2019.117645.

References

[1] R. von Burg, Inorganic mercury, J. Appl. Toxicol. 15 (1995) 483–493, https://doi.org/10.1002/jat.2550150610.
[2] H.H. Harris, The chemical form of mercury in fish, Science 301 (2003), https://doi.org/10.1126/science.1085941, 1203–1203.
[3] I. Onyido, A.R. Norris, E. Buncel, Biomolecule–Mercury interactions: modalities of DNA Base–Mercury binding mechanisms. Remediation strategies, Chem. Rev. 104 (2004) 5911–5930, https://doi.org/10.1021/cr030443w.
[4] U.S. Environmental Protection Agency, Ground water & drinking water, n.d, https://safewater.zendesk.com/hc/en–us/sections/202366308–Mercury. (Accessed 13 December 2018).
[5] M.Y. Chae, A.W. Czarnik, Fluorimetric chemodosimetry. Mercury(II) and silver(I) indication in water via enhanced fluorescence signaling, J. Am. Chem. Soc. 114 (1992) 9704–9705, https://doi.org/10.1021/ja00050a085.
[6] D.T. Quang, J.S. Kim, Fluoro– and chromogenic chemodosimeters for heavy metal ion detection in solution and biospecimens, Chem. Rev. 110 (2010) 6280–6301, https://doi.org/10.1021/cr100154p.
[7] J. Du, M. Hu, J. Fan, X. Peng, Fluorescent chemodosimeters using "mild" chemical events for the detection of small anions and cations in biological and environmental media, Chem. Soc. Rev. 41 (2012) 4511–4535, https://doi.org/10.1039/c2cs00004k.
[8] M.L. Turski, D.J. Thiele, New roles for copper metabolism in cell proliferation, signaling, and disease, J. Biol. Chem. 284 (2009) 717–721, https://doi.org/10.1074/jbc.R800055200.
[9] E. Gaggelli, H. Kozlowski, D. Valensin, G. Valensin, Copper homeostasis and neurodegenerative disorders (Alzheimer's, Prion, and Parkinson's Diseases and Amyotrophic Lateral Sclerosis), Chem. Rev. 106 (2006) 1995–2044, https://doi.org/10.1021/cr040410w.
[10] U.S. Environmental Protection Agency, Ground Water & Drinking Water, n.d, https://safewater.zendesk.com/hc/en–us/articles/211402978–4–What–are–EPA–s–drinking–water–regulations–for–copper–. (Accessed 13 December 2018).
[11] M.G. Choi, Y.J. Lee, I.J. Chang, H. Ryu, S. Yoon, S.K. Chang, Flatbed–scanner–based colorimetric Cu^{2+} signaling system derived from a coumarin–benzopyrylium conjugated dye, Sens. Actuators B Chem. 268 (2018) 22–28, https://doi.org/10.1016/j.snb.2018.04.068.
[12] Y. Wang, H. Wu, W.N. Wu, S.J. Li, Z.H. Xu, Z.Q. Xu, et al., An AIRE active Schiff base bearing coumarin and pyrrole unit: Cu^{2+} detection in either solution or aggregation states, Sens. Actuators B Chem. 260 (2018) 106–115, https://doi.org/10.1016/j.snb.2017.12.201.
[13] G. He, X. Liu, J. Xu, L. Ji, L. Yang, A. Fan, et al., Synthesis and application of a highly selective copper ions fluorescent probe based on the coumarin group, Spectrochim. Acta Part A Mol Biomol Spectrosc 190 (2018) 116–120, https://doi.org/10.1016/j.saa.2017.09.028.
[14] N. Mergu, M. Kim, Y.A. Son, A coumarin–derived Cu^{2+}–fluorescent chemosensor and its direct application in aqueous media, Spectrochim. Acta Part A Mol Biomol Spectrosc 188 (2018) 571–580, https://doi.org/10.1016/j.saa.2017.07.047.
[15] S.B. Warrier, P.S. Kharkar, A coumarin based chemosensor for selective determination of Cu (II) ions based on fluorescence quenching, J. Lumin. 199 (2018) 407–415, https://doi.org/10.1016/j.jlumin.2018.03.073.
[16] C. Li, Z. Yang, S. Li, 1,8–Naphthalimide derived dual–functioning fluorescent probe for "turn–off" and ratiometric detection of Cu^{2+} based on two distinct mechanisms in different concentration ranges, J. Lumin. 198 (2018) 327–336, https://doi.org/10.1016/j.jlumin.2018.02.031.
[17] S. Mukherjee, S. Hazra, S. Chowdhury, S. Sarkar, K. Chattopadhyay, A. Pramanik, A novel pyrrole fused coumarin based highly sensitive and selective fluorescence chemosensor for detection of Cu^{2+} ions and applications towards live cell imaging, J. Photochem. Photobiol. A Chem. 364 (2018) 635–644, https://doi.org/10.1016/j.jphotochem.2018.07.004.
[18] M. Pannipara, A.G. Al–Sehemi, M. Assiri, A. Kalam, A colorimetric turn–on optical chemosensor for Cu^{2+} ions and its application as solid state sensor, Opt. Mater. 79 (2018) 255–258, https://doi.org/10.1016/j.optmat.2018.03.051.
[19] J. Sun, X. Xu, G. Yu, W. Li, J. Shi, Coumarin–based tripodal chemosensor for selective detection of Cu(II) ion and resultant complex as anion probe through a Cu(II) displacement approach, Tetrahedron 74 (2018) 987–991, https://doi.org/10.1016/j.tet.2018.01.013.
[20] Y.-W. Wang, Y.-X. Hua, H.-H. Wu, X. Sun, Y. Peng, A solvent-tuning fluorescence sensor for In (III) and Al (III) ions and its bioimaging application, Chin. Chem. Lett. 28 (2017) 1994–1996, https://doi.org/10.1016/j.cclet.2017.07.019.
[21] Y.-W. Wang, S.-B. Liu, W.-J. Ling, Y. Peng, A fluorescent probe for relay recognition of homocysteine and Group IIIA ions including Ga (III), Chem. Commun. 52 (2016) 827–830, https://doi.org/10.1039/C5CC07886E.
[22] Z.-H. Fu, L.-B. Yan, X. Zhang, F.-F. Zhu, X.-L. Han, J. Fang, Y.-W. Wang, Y. Peng, A fluorescein-based chemosensor for relay fluorescence recognition of Cu (II) ions and biothiols in water and its applications to a molecular logic gate and living cell imaging, Org. Biomol. Chem. 15 (2017) 4115–4121, https://doi.org/10.1039/C7OB00525C.
[23] S. Mondal, C. Bandyopadhyay, K. Ghosh, Chromenone-rhodamine conjugate for naked eye detection of Al^{3+} and Hg^{2+} ions in semi aqueous medium, Supramol. Chem. 31 (2019) 1–8, https://doi.org/10.1080/10610278.2018.1522444.
[24] A. Majumdar, C.S. Lim, H.M. Kim, K. Ghosh, New six-membered pH-insensitive rhodamine spirocycle in selective sensing of Cu^{2+} through C–C bond cleavage and its application in cell imaging, ACS Omega 2 (2017) 8167–8176, https://doi.org/10.1021/acsomega.7b01324.
[25] K. Ghosh, T. Sarkar, A. Majumdar, Rhodamine-labeled Sensor Bead as a Colorimetric and Fluorometric Dual Assay for Hg^{2+} Ions in Water, Asian Journal of Organic Chemistry 2 (2013) 157–163, https://doi.org/10.1002/ajoc.201200134.
[26] K. Ghosh, T. Sarkar, A. Samadder, A.R. Khuda-Bukhsh, Rhodamine-based bis-sulfonamide as a sensing probe for Cu^{2+} and Hg^{2+} ions, New J. Chem. 36 (2012) 2121–2127, https://doi.org/10.1039/C2NJ40391A.
[27] Y. Gao, C. Zhang, S. Peng, H. Chen, A fluorescent and colorimetric probe enables simultaneous differential detection of Hg^{2+} and Cu^{2+} by two different mechanisms, Sens. Actuators B Chem. 238 (2017) 455–461, https://doi.org/10.1016/j.snb.2016.07.076.
[28] A.S. Murugan, M. Pandi, J. Annaraj, A Single and Simple Receptor as a Multifunctional Chemosensor for the Al^{3+}/Cu^{2+} ions and Its Live Cell Imaging Applications, Chemistry 2 (2017) 375–383, https://doi.org/10.1002/slct.201601646.
[29] S. Acharyya, S. Gharami, L. Patra, T.K. Mondal, An Efficient Fluorescence "Turn–On" Chemosensor Comprising of Coumarin and Rhodamine Moieties for $Al^{3+}$and Hg2+, J. Fluoresc. 27 (2017) 2051–2057, https://doi.org/10.1007/s10895–017–2144–9.
[30] X. Meng, S. Li, W. Ma, J. Wang, Z. Hu, D. Cao, Highly sensitive and selective chemosensor for Cu^{2+} and $H_2PO_4^-$ based on coumarin fluorophore, Dyes Pigments 154 (2018) 194–198, https://doi.org/10.1016/j.dyepig.2018.03.002.
[31] M. Guo, P. Dong, Y. Feng, X. Xi, R. Shao, X. Tian, et al., A two–photon fluorescent probe for biological Cu (II) and PPi detection in aqueous solution and in vivo, Biosens. Bioelectron. 90 (2017) 276–282, https://doi.org/10.1016/j.bios.2016.11.069.
[32] Q.H. You, A.W.M. Lee, W.H. Chan, X.M. Zhu, K.C.F. Leung, A coumarin–based fluorescent probe for recognition of Cu^{2+} and fast detection of histidine in hard–to–transfect cells by a sensing ensemble approach, Chem. Commun. 50 (2014) 6207–6210, https://doi.org/10.1039/c4cc00521j.
[33] A. Kumar, S. Mondal, K.S. Kayshap, S.K. Hira, P.P. Manna, W. Dehaen, et al., Water switched aggregation/disaggregation strategies of a

coumarin–naphthalene conjugated sensor and its selectivity towards Cu^{2+} and Ag^{+} ions along with cell imaging studies on human osteosarcoma cells (U–2 OS), New J. Chem. 42 (2018) 10983–10988, https://doi.org/10.1039/c8nj01631c.

[34] S. Park, H.–J. Kim, Highly selective and sensitive fluorescence turn-on probe for a catalytic amount of Cu(I) ions in water through the click reaction, Tetrahedron Lett. 53 (2012) 4473–4475, https://doi.org/10.1016/j.tetlet.2012.06.079.

[35] Y. Cho, K.H. Ahn, A 'turn–on' fluorescent probe that selectively responds to inorganic mercury species, Tetrahedron Lett. 51 (2010) 3852–3854, https://doi.org/10.1016/j.tetlet.2010.05.081.

[36] M. Dong, T.H. Ma, A.J. Zhang, Y.M. Dong, Y.W. Wang, Y. Peng, A series of highly sensitive and selective fluorescent and colorimetric "off–on" chemosensors for Cu (II) based on rhodamine derivatives, Dyes Pigments 87 (2010) 164–172, https://doi.org/10.1016/j.dyepig.2010.03.015.

[37] M. Santra, D. Ryu, A. Chatterjee, S.K. Ko, I. Shin, K.H. Ahn, A chemodosimeter approach to fluorescent sensing and imaging of inorganic and methylmercury species, Chem. Commun. (2009), https://doi.org/10.1039/b900380k, 2115–7.

[38] Y. Xiang, A.J. Tong, P.Y. Jin, Y. Ju, New Fluorescent Rhodamine Hydrazone Chemosensor for Cu (II) with High Selectivity and Sensitivity, Org. Lett. 8 (2006) 2863–2866, https://doi.org/10.1021/ol0610340.